ARTICLE IN PRESS

Journal of Cleaner Production xxx (xxxx) xxx

EI SEVIER

Contents lists available at ScienceDirect

Journal of Cleaner Production

journal homepage: www.elsevier.com/locate/jclepro



Parametric life cycle assessment for distributed combined cooling, heating and power integrated with solar energy and energy storage

Junchen Yan a, *, Osvaldo A. Broesicke a, Dong Wang a, **, Duo Li b, John C. Crittenden a

ARTICLE INFO

Article history: Received 27 July 2019 Received in revised form 25 November 2019 Accepted 26 November 2019 Available online xxx

Handling Editor: Sandro Nizetic

Keywords:
Parametric life cycle assessment
Distributed energy production
Combined cooling heat and power
Renewables
Energy storage
Integrated system
Life cycle cost

ABSTRACT

In this research, we develop a parametric life cycle assessment framework and evaluate the environmental and economic trade-offs of a distributed combined cooling, heating, and power system integrated with renewable energy and energy storage system (CCHP-RE-ESS). Also, we compare this to centralized conventional energy generation. The CCHP-RE-ESS system consists of microturbines, solar PVs, lithiumion batteries, and other auxiliary system components. Using a parametric life cycle assessment approach, we learn the trade-offs environmental and economic impacts for various sizes of solar PVs arrays and batteries. The emission impact result from the parametric life cycle assessment is more accurate than the conventional life cycle assessment due to hourly-based simulation and parametric models for different system components. Our simulations show that the proposed system that follows the thermal load can primarily reduce the overall environmental impact as compared to the centralized conventional energy production for most building types and climate zones we studied. For example, the system can help a medium office in Atlanta reduce 46% of global warming impact, 98% of water usage, 93% of acidification impact, etc. In terms of cost, the life cycle cost of the proposed system is often higher than conventional energy generation while it is more economical for the small and large office than the medium office.

© 2019 Elsevier Ltd. All rights reserved.

1. Introduction

Driven by rapid economic and population growth in the past few decades, cities consume over two-thirds of the world's energy and account for more than 70% of global CO2 emissions (Arup, 2018). The United Nations and International Energy Agency estimate that the continuing urbanization and growth of the world's population is projected to add 2.5 billion people to the urban population and a 70% increase in energy demand by 2050 (United Nations, 2014). The increase in energy consumption will cause more energy-related water usage, as well as carbon dioxide and pollutant emissions. Cities are looking for a more efficient and less polluting way to meet the increasing energy demand.

Trigeneration or combined cooling, heat and power (CCHP) as a distributed energy generation solution (Darrow et al., 2017) has

E-mail addresses: junchen.yan@gatech.edu (J. Yan), dwang473@gatech.edu (D. Wang).

https://doi.org/10.1016/j.jclepro.2019.119483 0959-6526/© 2019 Elsevier Ltd. All rights reserved. higher efficiency than conventional energy generation because waste heat can be recovered and used to meet the heating and cooling loads. Besides, the distributed energy generation system is closer to the end-users and hence can avoid energy transmission losses. Recent studies have shown that integrating the CCHP with renewable energy and energy storage device can help to further enhance local power reliability and sustainability performance (e.g. less energy-related emissions and water usage) (Faisal et al., 2018).

Previous research studies evaluated different aspects and system configurations (the combination of technologies) of the distributed CCHP energy system integrated with renewable energy and energy storage (CCHP-RE-ESS). Rastegar et al. (Rastegar and Fotuhi-Firuzabad, 2015) proposed an optimization-based program to determine the optimal operation mode of a residential energy hub consisting of plug-in hybrid electric vehicles, combined heat and power, solar panels, and electrical storage system. Rodriguez et al. (Rodríguez et al., 2016) assessed the performance of several designs of hybrid systems composed of solar thermal collectors, photovoltaic panels and natural gas internal combustion engines. A calculation is performed by Brandoni et al. (Brandoni and Renzi, 2015) to illustrate the optimal sizing of a hybrid renewable

^a Brook Byers Institute for Sustainable Systems, School of Civil and Environmental Engineering, Georgia Institute of Technology, 828 West Peachtree Street, Suite 320, Atlanta, GA, 30332-0595, USA

^b International Alliance on Environmental Protection and Sustainable Development Inc., USA

^{*} Corresponding author.

^{**} Corresponding author.

system made up of an electrical solar device and a micro-Combined Heat and Power (CHP).

The results of Shah et al. 's (Shah et al., 2015) research provided guidance for both design and deployment of PV, battery, and CHP hybrid systems in any continental American to reduce consumer costs, while reducing energy- and electricity-related emissions. Maleki et al. (2017) introduced an economic optimization model method for the performance of grid-connected hybrid CHP systems using solar, wind and fuel cell technologies for residential uses. A co-constrained multi-objective particle swarm optimization algorithm is applied for optimal cost savings of a CCHP system including photovoltaic modules, wind turbines, and solid oxide fuel cells (Soheyli et al., 2016).

Mohammadi et al. (Mohammadi et al., 2017) conducted an energy and exergy analyses for a CCHP cycle comprised of a gas turbine and absorption refrigeration system integrated with wind energy coupled with compressed air energy storage. Balcombe et al., 2015b evaluated the life cycle environmental impact for a microgeneration system combining solar PV, CHP plant and battery storage a household energy demand. Mehrpooya et al. (2017) investigated the process performance of an integrated CCHP plant, which consists of molten carbonate fuel cell, Stirling engine and gas turbine and double-effect LiBr/H₂O absorption chiller by sensitivity analysis of the effective parameters.

By and large, few research studies conducted cradle-to-grave life cycle assessment studies on CHHP-RE-ESS. The life-cycle assessment (LCA) of CCHP-RE-ESS for commercial building energy supply is scant, especially in the U.S. context (U.S. Department of Energy, 2018; Balcombe et al., 2015b). Besides, the performance and emission of different CCHP-RE-ESS technologies depend on their operation conditions such as ambient temperature, sizes, and part load ratio. For example, the emission of microturbine per kWh of energy generated is a function of ambient temperature and part load ratio as reported by the manufacturers. However, LCA study conducted by Balcombe et al., 2015a, 2015b only consider average emission data and reports case-specific impact results. They failed to show why and how much results vary with different conditions (e.g., energy demand profiles, system component sizes, operating conditions). Compared to conventional LCA, the parametric LCA is more accurate since it reveals how and why impact changes with different operating conditions (Lee and Thomas, 2017).

In this research, a novel distributed CCHP-RE-ESS configuration which consists of microturbines, a heat recovery unit, an adsorption chiller, solar panels, and lithium-ion batteries for different building types and locations is studied and evaluated for different building types ar various climate zones. We used a new approach, the parametric cradle-to-grave life cycle assessment to evaluate the environmental and economic impact of the proposed system. The impact results are finally integrated with a multi-objective optimization method, Pareto front, to find the optimal environmental and economic impact trade-offs for different building types at various climate zones. We used MATLAB (The MathWorks, Inc.) to develop our parametric and optimization evaluation model.

2. Methods

2.1. The system framework configuration

Fig. 1 shows the system configuration of the proposed system versus conventional energy generation. In the US, the conventional energy generation for buildings are comprised of electricity from the central electricity grid and heat from a furnace or boiler (Betz, 2009), cooling demand is met by air conditioner powered by electricity. The CCHP-RE-ESS system is composed of a prime mover,

a heat recovery unit, an absorption chiller, a set of renewable energy sources, an energy storage device, and electrical interconnections.

2.2. Goal and Scope

The goal of life cycle assessment (LCA) is to compare the proposed system with various conventional energy generation in terms of economic cost, freshwater consumption, air emissions impacts (i.e., acidification, eutrophication, ecotoxicity, global warming, etc.) for various climatic conditions and building types.

2.3. Functional unit

The functional unit is the annual impact of the energy generation system to meet the energy demand of one foot square of the building (impact per foot square). Since the energy demand profile of buildings in different clime zones varies, we use impact per foot square as the functional unit rather than impact per kWh. The service life of the proposed system is 20 years.

2.4. System boundary

As shown in Fig. 2, our cradle-to-grave LCA for the proposed system mainly includes three stages: (1) hardware manufacturing, (2) operation & maintenance (O & M), and (3) end-of-life treatment. We excluded components related to building electrical interconnections, construction, and operations because these would be similar for the centralized and decentralized systems. We used process-based LCA for most of the stage processes. The economic input-output-based (EIO) methods (Yang et al., 2017) was only for determining the impact during routine maintenance. The U.S. Life Cycle Inventory Database (U.S. Life Cycle Inventory Database, 2012) process-based inventory data was used for on-site power generation and end of life treatment. For product manufacturing, pipeline natural gas, and end-of-life waste disposal, we used the inventory from the Ecoinvent 3 database in Simapro 8 (PRe North America Inc, 2017).

For EIO, a new and transparent the United States Environmentally Extended Input-Output Model (USEEIO) (Yang et al., 2017) was adopted. This model melds data on economic transactions between 389 industry sectors with environmental data for these sectors covering water, energy and mineral usage and emissions of greenhouse gases, criteria air pollutants, nutrients and toxics, to build a life cycle model of 385 US goods and services.

For conventional energy generation, the United States uses different types of energy sources. By and large, fossil fuels have dominated the energy mix. The energy-related emissions can also vary due to different energy mixes of each state. The grid emissions data were obtained from the Emissions and Generation Resource Integrated Database (eGRID). We calculated state-level emission information as the inventory of conventional electricity supply. Since eGRID's emissions are measured at the sources and do not account for losses from transmission and distribution infrastructures. We assumed a 7% transmission loss (Lee, 2017). The emission inventory of different states (involved in this study) for conventional energy is presented in Table S2. We also evaluated the process-based impact for power plant construction and decommissioning via Simapro 8.

2.5. Life cycle impact inventory

The life cycle emissions inventory includes greenhouse gases (GHGs - CO2, N2O, and CH4), carbon monoxide (CO), ammonia

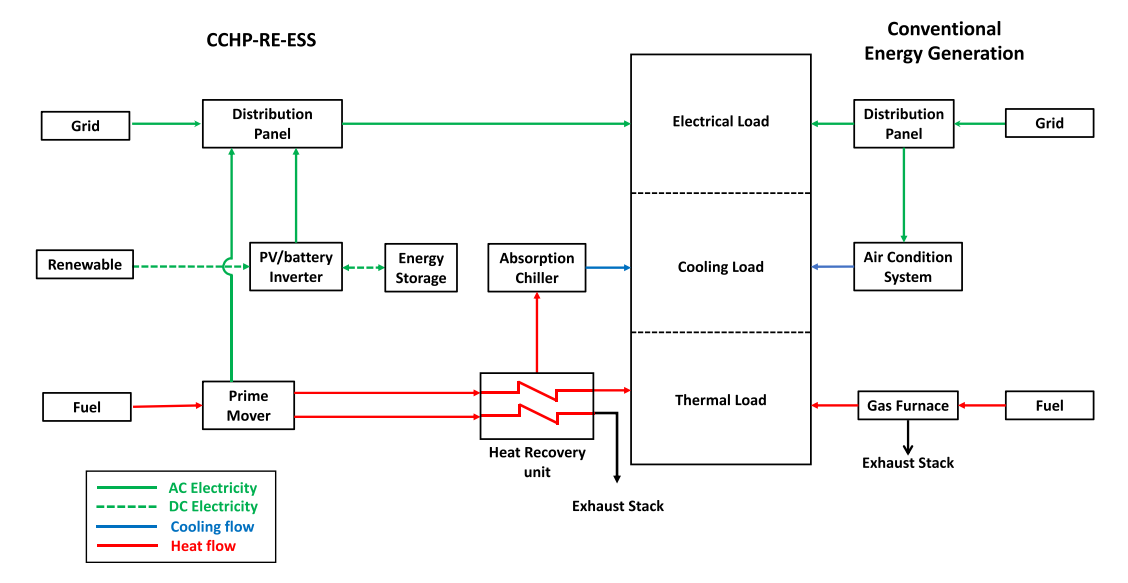


Fig. 1. System Configuration.

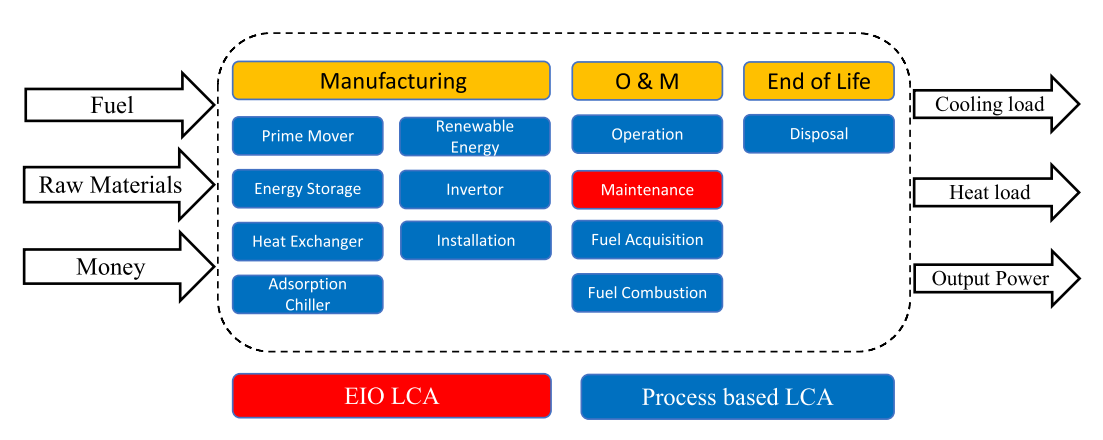


Fig. 2. System boundary.

(NH3), nitrogen oxides (NOx), particulate matter (PM2.5 and PM10), sulfur dioxide (SO2), and volatile organic compounds (VOCs). We assessed their midpoint life cycle environmental impacts – climate change, acidification, eutrophication, ecotoxicity, ozone depletion and fossil fuel depletion based on TRACI 2.1 (Bare, 2001). The life cycle water consumption was presented in gallons of freshwater used. We normalized the environmental impact to a percentage by dividing the impact by the average impact of a US resident. For the US, total and per-capita year normalization factors have been published for use in the TRACI 2.1 LCIA model (Ryberg et al., 2014) as shown in Table S2. The normalized mid-point impact results are multiplied by the weighting factors to generate a single overall score. We used the environmental impact importance weights developed by the Analytic Hierarchy Process (AHP) technique at the panel event (Ryberg et al., 2014). The weighting factors are tabulated in Table S3.

2.6. Economic life cycle cost

We broke all costs of the proposed system into two main categories: fixed costs and variable costs. Fixed costs are costs that are independent of output, while variable costs are costs that vary with amount of energy required. For the CCHP-RE-ESS, fixed costs

include purchase for prime mover, renewable energy, energy storage device, heat recovery unit, absorption chiller, other auxiliary system components, and installation service (Baer et al., 2015). Fixed cost of conventional energy supply consisting of the construction of power generation and transmission infrastructures and is assumed to be included in the electricity and heating service fees.

Variable costs of the proposed system include purchase for fuel, operation and maintenance service. Variable costs of the conventional energy system include purchases for electricity and heating. The cost inventory is shown in Table S4. All monetary values are in constant 2019 dollars in net present value over 20 years of system lifetime, at a 7% discount rate. Equations (1) and (2) shows the average annual LCC for conventional and proposed system respectively.

$$LCC_{CE} = \sum \frac{C_{Electricity} + C_{Fuel}}{(1+r)^{i} \times 20 \times FA}$$
 (1)

$$LCC_{CCHP-RE-ESS} = \sum \frac{C_{IV} + C_{Electricity} + \frac{C_{Fuel}}{(1+r)^i}}{20 \times FA}$$
 (2)

Where i stands for i-th year, LCC is life cycle cost in dollars per

4

square foot, C is cost in dollars, r is discount rate. FA is the building floor area in square foot.

2.7. System operation and sizing

The microturbine was designed to be a "follow the thermal load (FTL)" model since previous research studies show that systems of this type have lower emissions than following the electrical load of the building (Mago et al., 2009; Mago and Chamra, 2009). To be more specific, microturbine generates more heat than electricity, and "follow the electric load (FEL)" will produce more heat than what can be used by the building. For the system that used only CCHP and FEL, extra electricity comes from the grid. The integration of renewable energy and energy storage can help increase off-grid electricity generation.

Hence, the selection of microturbine size is based on the maximum hourly thermal energy required by the building. The absorption chiller for each building was sized to satisfy the cooling requirement of the building. Sizes of energy storage and solar energy can vary, we plotted the Pareto front to find the optimal size combinations. The maximum energy storage capacity is limited by maximum daily electricity demand and the maximum usable roofing area for solar PV is assumed to be 80 percent of the total roof area.

2.8. Dispatch strategy

The electricity control dispatch strategy for the proposed system, shown in Fig. 3. This is the priority for electricity dispatch: first is the prime mover, second is renewable energy, third is energy

storage, and finally the grid in order. If the electricity demand is fulfilled, the remaining energy is stored in the energy storage device if it is not fully charged. The energy stored in the battery will be used during times when there is insufficient electricity generated from the prime mover and renewable energy to match the electrical demand. Due to electrical current and voltage constraints, the battery can only be charged by solar panels. If the battery is fully charged, extra electricity produced is assumed to be wasted. We did not consider net metering in this research since some states in the US had sustainable energy generation rules other than net metering.

2.9. Building energy demand simulation

We used EnergyPlus (U.S. DOE, 2019) to model the building energy consumption for heating, cooling, ventilation, lighting, plug loads, etc. According to the National Renewable Energy Laboratory and U.S. DOE, 16 building types represent approximately 70% of the commercial buildings in the U.S. (U.S. DOE and National Renewable Energy Laboratory, 2011). These buildings' characteristics were modeled into the commercial reference benchmark models developed by DOE. We incorporated the commercial reference benchmark models and TMY3 weather file (Torcellini et al., 2008) to the EnergyPlus simulation software to provide energy demand for different types of buildings (Table S5) at 16 clime zones (Table S6) in the U.S.

The simulation provides hourly-based energy demand data in terms of electricity for appliances and natural gas for heating. Equations (3) and (4) calculate the conventional electrical and thermal energy demand for buildings. Facilities powered by

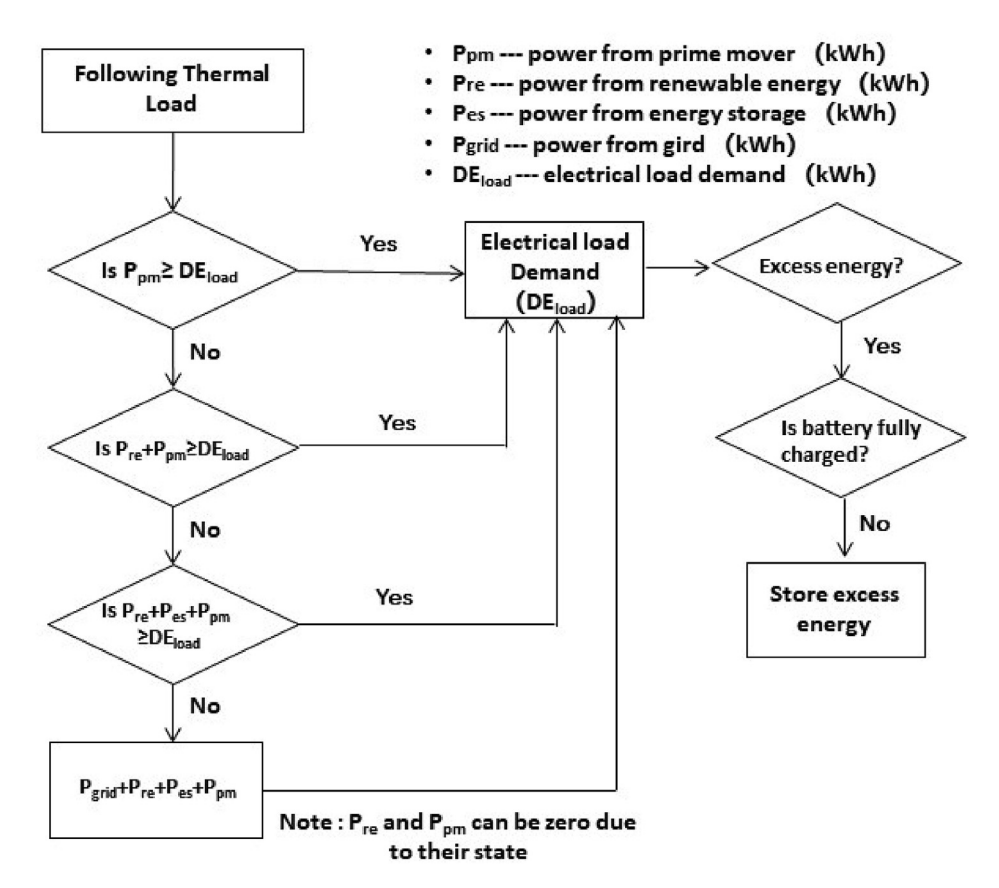


Fig. 3. Dispatch strategy.

electricity include air conditioning systems, fans, pumps, lights, and other plug loads. The thermal demand for space heating and hot water is met by gas furnace fueled by natural gas. Some types of buildings (e.g. medium office) use electricity to meet part of its heating demand.

$$E_{CE} = E_{PlugLoads} + E_{AirConditioning}$$
 (3)

$$Th_{CE} = Th_{Heating} + Th_{HotWater}$$
 (4)

Where E stands for electrical energy (kWh), Th stands for thermal energy (kWh).

Equations (5) and (6) determine the energy generation when buildings use the CCHP-RE-ESS. In this case, the air conditioning system is substituted by the absorption chiller that can convert heat into cooling power. The amount of heat needed by the absorption chiller is determined using the ratio of the coefficient of performance (COP) of the air conditioner and absorption chiller. The COP of the air conditioning units was assumed to be 3.8, and the COP of a double effect absorption chiller used is 1.42 [51,65] (K.T.E.Co, 2008).

$$E_{CCHP-RE-ESS} = E_{PlugLoads} \tag{5}$$

$$Th_{CCHP-RE-ESS} = Th_{Heating} + Th_{HotWater} + \frac{COP_{AirConditioning}}{COP_{AdsorptionChiller}} \times E_{AirConditioning}$$

$$(6a)$$

2.10. Parametric framework

To account for nonlinear and varying performances of different components of the proposed CCHP-RE-ESS system, we developed submodule for three categories of commercially available technologies into the proposed energy generation system: (1) a microturbine for prime mover; (2) lithium-ion batteries for energy storage and (3) solar PVs for renewable energy.

For prime mover, the Capstone air-cooled microturbines (Van Nuys, Los Angeles) were chosen for this study as they use air-cooling rather than water-cooling (James et al., 2016). The performance of the microturbine depends on factors such as ambient temperature, altitude, power output ratio. According to a manufacturer's data (Capstone Turbine Corporation, 2009)., a higher power output ratio results in higher efficiency and lower emissions. We used multiple non-linear regression to develop a model that can predict fuel consumption and emission for a C200 microturbine-based on manufacture data. Equation (7) shows the objective function of the regression. Due to the lack of pressure data, the equation only estimates the fuel consumption based on ambient temperature and power output ratio under standard atmosphere. The parameter value and objective function are shown in Table S7.

$$FC_M = \beta_1^{(1-PL)} \times \beta_2 \times T \tag{6b}$$

$$OF = \sqrt{\frac{1}{n-1} \times \sum (\frac{FC_{DA} - FC_{SIM}}{FC_{SIM}})^2}$$
 (7)

Where FCM is the fuel consumption of microturbine (MJ), β is the regression coefficient, T is ambient temperature (K), PL is part-load ratio or power output ratio (%). Where n is the number of data points, and FCData and FCSIM (MJ) are manufacture data and

simulation data.

For the solar energy submodule, we incorporated a more accurate and technical rigorous PV performance model that was developed by Sandia National Laboratories (National Technology and Engineering Solutions of Sandia, LLC., 2018). The model includes 5 components: (1) weather and system design, (2) singe module DC output. (3) array DC output. (4) DC to AC conversion and (5) AC output. The final power generation and losses depend on parameters such as temperature, location, array orientation, time, weather, etc. The PV system was designed using polycrystalline silicon PV cells mounted at a 30-degree angle towards the south and a peak power factor of 0.2 kW/m2. The unit size is 1.68m2 per panel. According to the NABCEP PV resource guide (Brooks and Dunlop, 2012), we assumed 80% of the roof area that has a suitable orientation can be used for mounting modules when room for maintenance, wiring paths, firefighter access (International Fire Code, 2012) and aesthetic considerations are considered. The average power output for each square meter of the usable roof area is 0.2 kW (Brooks and Dunlop, 2012). We calculated the minimum required distance between PV arrays using a separation factor of 2 from the NABCEP PV resource guide (Brooks and Dunlop, 2012). The maximum useable roofing area for the PV is assumed to be 80% of the total roof area.

For energy storage systems, the Li-ion batteries have been deployed in a wide range of energy-storage applications, ranging from a few kilowatt-hours in residential systems with rooftop photovoltaic arrays to multi-megawatt containerized batteries for the provision of grid-level storage. Hence, we choose the Tesla Powerpack as the energy storage for the proposed system. The energy capacity for each power pack is 210 kWh (AC) with a roundtrip efficiency of 90% (International Fire Code, 2012). The maximum power output is 50 kW per power pack. One of the major lithiumion battery disadvantage for consumer electronics is the aging of lithium-ion batteries in which the power storage and round-trip efficiency are reduced. This depends on the charging and discharging operation and the number of charge-discharge cycles that the battery has undergone. The battery in the proposed system is charged and discharged once per day. According to Tesla Powerwall 2 (2170 cell) warranty, there is a 70% capacity after 10 years (Tesla, 2017). We assumed EES technologies are replaced entirely for each ten years and the battery performance deteriorates in a linear fashion for 10 years.

2.11. Environmental and economic trade-offs

The multi-objective optimization is performed utilizing single score indicators, which can include several normalized and weighted impact categories. Every point represents a situation of energy generation using different sizes of solar PVs and batteries. For each point, there are two objective functions: life cycle single score environmental impact and the life cycle cost in net present value. The meaning of the Pareto front is that elements that are not on the front are never the best choice because there is some element on the front which is better. Moreover, designs that are on the front are the best choice. By considering all of the potential solutions, we can focus on tradeoffs between LCC and LCA.

2.12. Variability and uncertainty

Unlike traditional LCA, our parametric LCA framework considers the environmental impact and economic cost based on the hourly variability of the energy dispatch and not on just a single average value for the year. It can explain how and why the result varies with system conditions and weather. The environmental and economic impacts depend on energy generation and demand that vary with numerous factors (e.g. weather, building type, sizes, etc.). In addition, the input data can have uncertainty. The single value of each input, such as product price, maintenance cost, emissions was determined from the literature or manufacturer's guide. A sensitivity analysis was conducted to understand the impacts of variations in key parameters including turbine emission, and prices for EIO-LCA.

For the conventional energy system, we also considered the variation in the energy mix and its influence on the impact reduction of the proposed system. For example, the current energy mix of Arizona is composed of natural gas (42.5%), coal (16.0%), nuclear (26.9%), hydro (6.0%), other renewables (7.8%), whereas the energy mix of Georgia is composed of coal (67%), nuclear (21%), natural gas (10%), and hydro (2%) (EIA, 2019). The difference in the energy mix (emissions) results in a difference in baseline conditions when we compare the impact of the proposed system with conventional energy supply.

3. Results and discussion

3.1. Life cycle assessment and costs

By using our parametric framework, we simulated the energy generation and supply of a medium office in Atlanta for the proposed system. The global warming impact and water consumption of a medium office in Atlanta with different sizes of solar and energy storage are shown in Fig. 4. Other impact categories, including acidification, eutrophication, ecotoxicity, ozone depletion, and fossil fuel depletion, are shown in Fig. S1. As shown in Fig. 4, compared to conventional energy generation in Atlanta, Georgia (32 kg CO2 eq per ft2 and 2.59-gal water per ft2), the integrated solar and energy storage system can further decrease the global warming impact by 21–46%, the water consumption by 70%–98%. The proposed system also reduces the acidification and fossil fuel depletion impact by 52–93% and 67–91%, respectively. On the other hand, the ozone depletion, ecotoxicity, and eutrophication impact are higher than conventional energy supply. The ecotoxicity

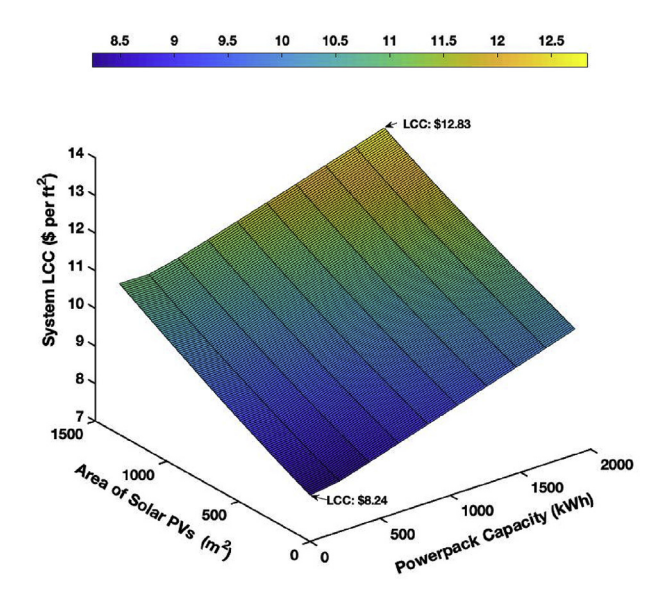


Fig. 5. Life cycle cost of the proposed system for a medium office in Atlanta.

and eutrophication impact increases with solar and battery sizes since the impacts are generated during the product manufacturing stages.

The life cycle cost per functional unit is shown in Fig. 5, the annual average price (electricity, heating, and cooling) for conventional energy supply is about 2.58 dollars per square feet as compared to \$8 to \$13 for the proposed system. The life cycle cost depends on how many solar panels and battery installed. Unlike most turbines for CCHP in the market, the maintenance cost of Capstone microturbine is just about 0.003 per kWh because of their air bearing technology. The higher marginal cost is useful for policymakers and other stakeholders to implement policy incentives. Admittedly, net metering can help to reduce the cost. However, in this case, selling energy back to the grid is not considered since Georgia Power did not offer a net energy metering tariff currently. Besides, the cost of the conventional energy system also varies with

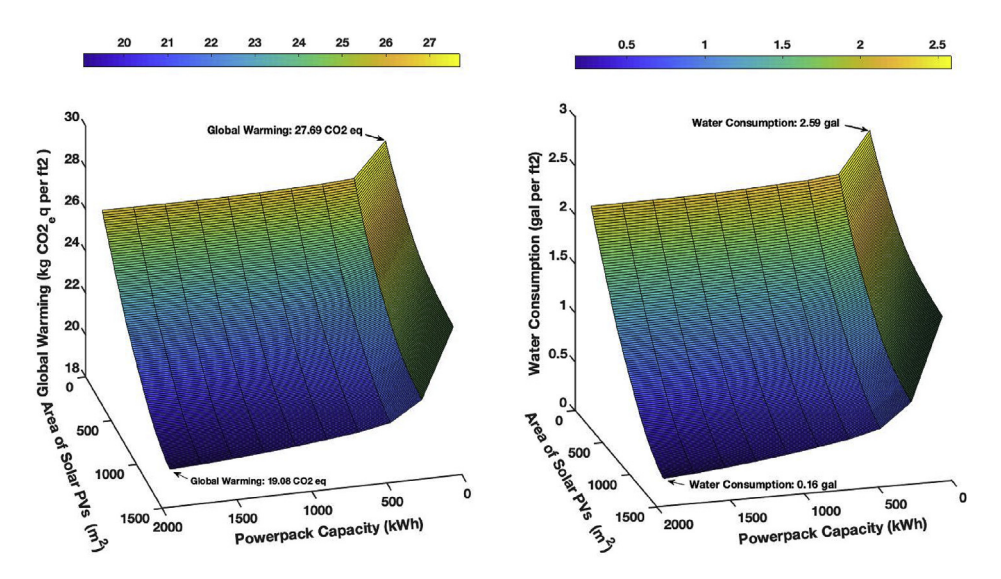


Fig. 4. The global warming impact and water consumption of the CCHP system for a medium office in Atlanta. For conventional energy, the global warming impact is 35 CO2 eq per ft2 and water consumption is 8.7 gal per ft2.

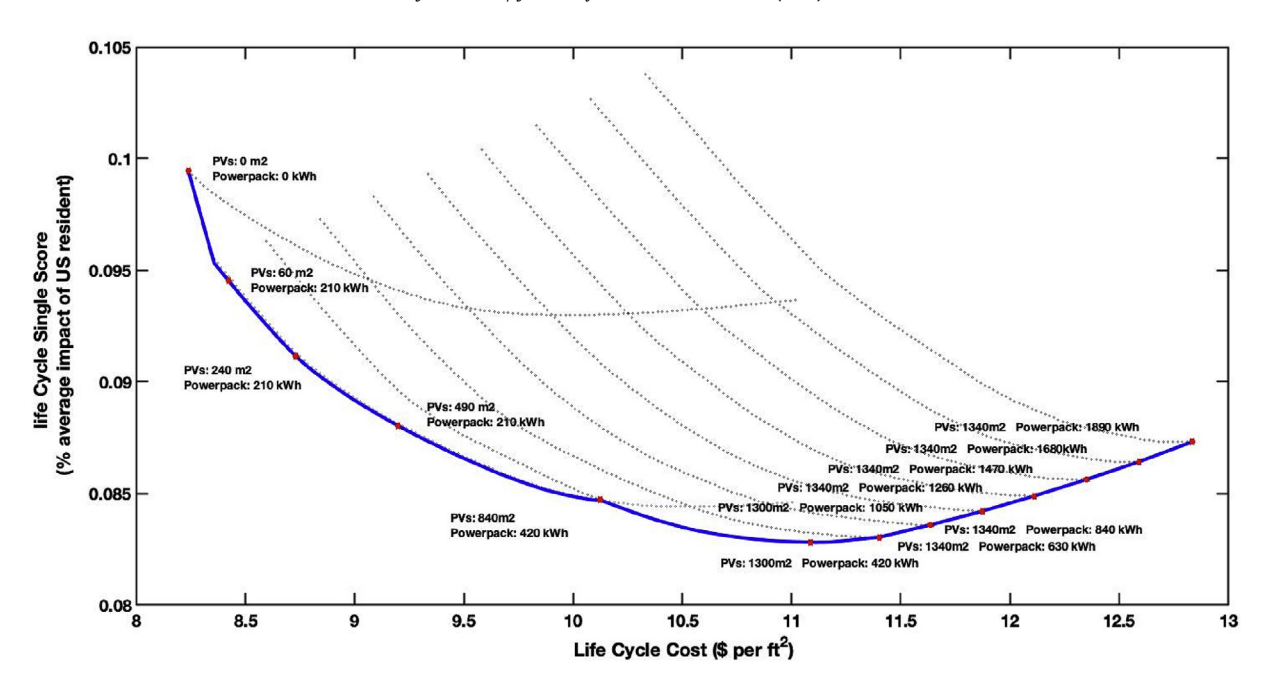


Fig. 6. The Pareto front for different system sizes.

geospatial conditions.

3.2. Environmental and economic trade-off

As discussed, impacts and costs vary with PVs and batteries sizes. We created a Pareto front to find the optimal systems for hundreds of scenarios (building types and locations). The resulting Pareto front provides an approximation of all efficient solutions which can then be selected for detailed analyses. The Pareto front for Atlanta medium office is shown in Fig. 6. The single score impact first reduces as the cost increases. After reaching its minimum, it starts to increase again which means the renewable system benefits have reached its maximum and increasing sizes will cause more impact because of the impacts of manufacturing. We choose the minimum environmental impact as our optimal solution. The corresponding sizes are 1300 m² of solar panels, 420 kWh battery or two battery packs. The optimal sizes for other system components for different building types and locations are shown in Table S8.

3.3. Power generation

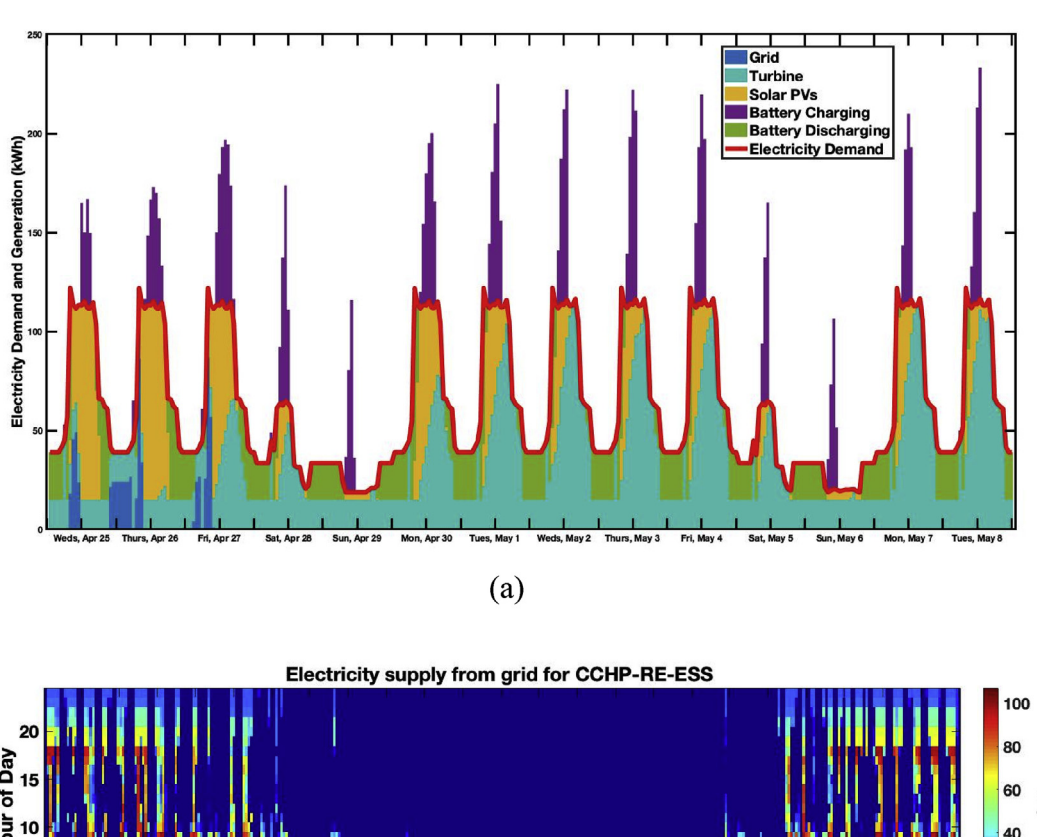
Fig. 7a shows the optimal scenario 14 days' power generation and energy demand of (from Wednesday, April 25th to Tuesday, May 8th) the proposed system for Atlanta medium office building. Fig. 7b shows the annual power generation from the grid with and without the CCHP-RE-ESS. The energy demand and corresponding generation of weekends are much lower than weekdays (Fig. 7a) since the studied building is an office that has less activity on the weekend. The battery system is charged during the day and discharges at night and before dawn. As shown in both Fig. 7 a and b, at the end of April, the building requires a few electricity from the grid, and after April 27th, the building can be completely off-grid until early September. This is because, in summer, the thermal demand is high (heating and cooling), by following thermal load, the electricity from microturbine is enough for daytime demand, and power from PV fully charge the battery. In total, the system can meet more than 90% of electricity demand for the building (turbine: 58%, solar and storage: 34%, and grid: 8%). Detailed system components electricity supply proportions of CCHP-RE-ESS for studied building types and locations are reported in Table S9.

3.4. Building types and location

The optimal US annual per capita environmental LCA single scores and LCC of the proposed system and local conventional energy generation is shown in Figs. 8-9. Fig. 8 shows LCA single scores and LCC of a medium office in different weather zones. The single scores of CCHP-RE-ESS for medium offices are lower than the local conventional energy supply impact score except for Phoenix. There are not very much different for the single scores and cost of the proposed system for the medium office at Atlanta, Chicago, Duluth, and Miami. Phoenix medium office has the highest environmental single score and life cycle cost. According to Fig. 9, for different building types in Atlanta, the large office has the lowest cost and the small office has the lowest single score. Compared to single the score of conventional energy generation, the medium office has the largest benefit by adopting CCHP-RE-ESS (30% reduction in overall impact). On the other hand, the single score of CCHP-RE-ESS for the large office is nearly the same as the score of conventional energy generation. From these results, the majority of the resulting impact and cost for our decentralized system is due to natural gas emissions from the turbine. We also conduct a sensitivity analysis of natural gas consumption and emission. According to the range shown in Figs. 8–9, the final impact can vary by about 20%. For each scenario, the specific environmental impacts under optimal situations are reported in Table S10. The environmental impacts for conventional energy generation in different states are reported in Table S11. Detailed cost proportions (investment, grid electricity, fuel, and maintenance cost) for LCC are reported in Table S12.

4. Conclusions

In this study, we developed a parametric life cycle assessment framework by MATLAB and evaluated the environmental and economic impact of a distributed CCHP-RE-ESS consists of



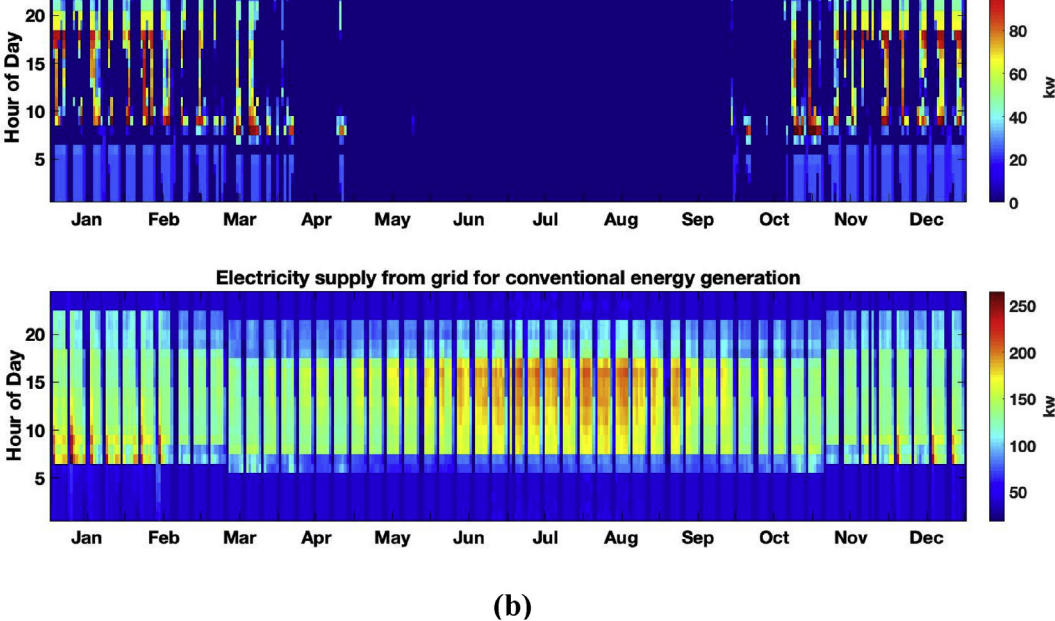


Fig. 7. Power generation for electricity demand of a medium office in Atlanta: (a) 14 days (Wednesday, April 25th to Tuesday, May 8th) electrical power generation of the CCHP-RE-ESS system. (b) Annual electricity from gird (conventional energy generation and CCHP-RE-ESS scenarios).

microturbines, solar PVs, lithium-ion batteries, and other auxiliary system components. We used a multi-objective optimization method, Pareto front, to find the optimal environmental and economic impact trade-off and corresponding solar and battery sizes for different commercial building types at various climate zones. The simulation results showed that the CCHP-RE-ESS and proposed technologies have less life cycle environmental impact compared to conventional power generation. By adopting the proposed system, buildings require much less electricity demand from the grid. For example, it has been shown that the proposed system could help a medium office in Atlanta save 21–46% of global warming impact and 70%–98% of water usage at different sizes of solar PVs and

lithium-ion batteries. The distributed CCHP-RE-ESS can also stay more than 90% off-grid by following the thermal load of a medium office. One disadvantage of the CCHP-RE-ESS system is the higher life cycle cost compared to the conventional energy supply. From the results, the medium office building can have the largest environmental benefit by adopting the CCHP-RE-ESS.

Besides, the new parametric life cycle assessment framework developed in this research is more accurate compared to the conventional life cycle assessment. The parametric LCA can explain how impacts change with different inputs under various scenarios rather than average values reported by conventional LCA. Future works include parametric models for more technologies such as

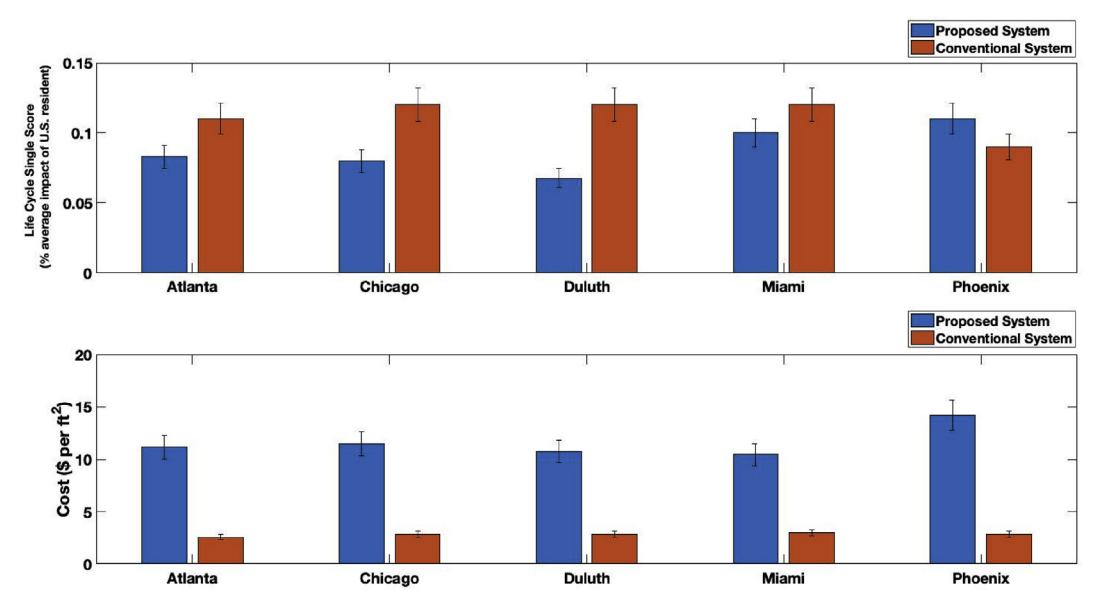


Fig. 8. Comparison for medium office building for different locations.

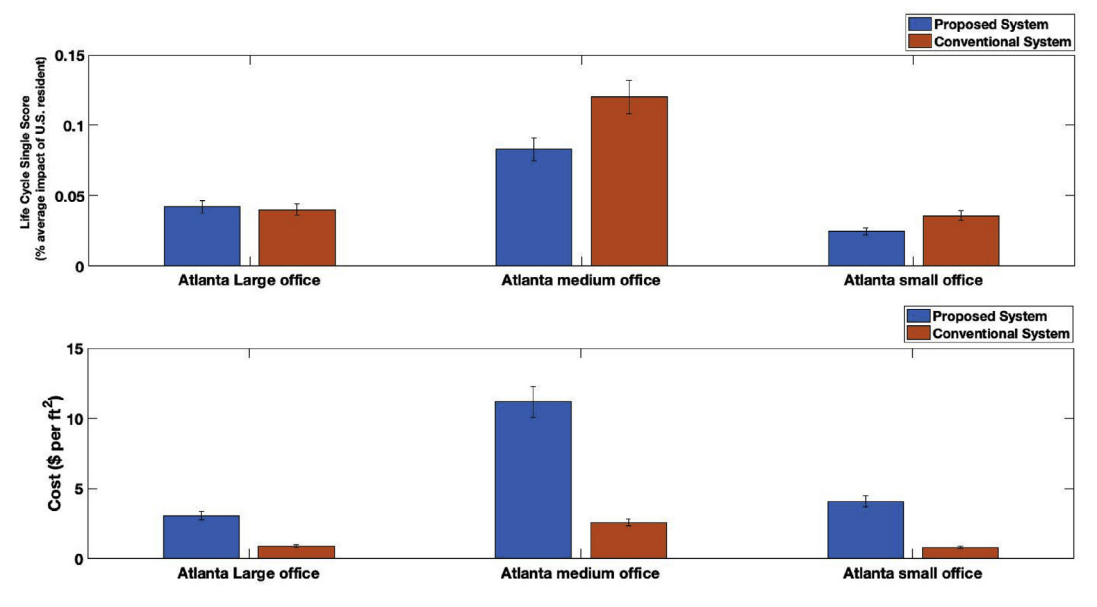


Fig. 9. Different building types in Atlanta.

fuel cells as a prime mover, wind energy as a renewable energy source, and compressed air energy storage. Overall, the distributed CCHP-RE-ESS with proposed technologies is a more efficient and environmentally friendly way to meet the increasing urban energy demand. The technologies combination of this study offers a cleaner energy production by reducing the overall life cycle impact.

Contributions

Junchen Yan: Developing the parametric LCA model, Original draft preparation, Writing, and Editing. **Osvaldo A. Broesicke:** Performing the PVPerformance model developed by Sandia National Laboratories. **Dong Wang:** Reviewing and Editing, Air pollution inventory. **Duo Li:** Comments and suggestions on the life cycle cost section. **John C. Crittenden:** First author's Ph.D. advisor, Reviewing, and Editing.

Declaration of competing interest

The authors declare that they have no known competing financial interests or personal relationships that could have appeared to influence the work reported in this paper.

Acknowledgements

The authors appreciate the support from the Brook Byers Institute for Sustainable Systems, Hightower Chair, and Georgia Research Alliance at the Georgia Institute of Technology. This work was also supported by the grant for "EAGER: SSDIM: Superimposed Simulations: Fast Generation of Synthetic Data of Interdependent Critical Infrastructures" (#1745580) from the National Science Foundation, Division of Civil, Mechanical, & Manufacturing Innovation (CMMI). The views and ideas expressed herein are solely

10

those of the authors and do not represent the ideas of the funding agencies in any form.

Appendix A. Supplementary data

Supplementary data to this article can be found online at https://doi.org/10.1016/j.jclepro.2019.119483.

Nomenclature

Abbreviations and symbols

AC alternating current
AHP analytic hierarchy process
CHP combined heating, and power

CCHP combined cooling, heating, and power

CCHP-RE-ESS combined cooling, heating, and power integrated

with renewable and energy storage system

C(\$) cost

COP coefficient of performance

DC direct current
E (kWh) electricity demand

r (%) discount rate

eGrid Emission & Generation Resource Integrated Database

ELCA environmental life cycle assessment

FA (ft2) build floor area

FEL following the electric load

FC (MJ) Fuel Consumption

FTL following the thermal load LCA life cycle assessment

LCC (\$/ft2) life cycle cost

n number of manufacture data

OF objective function

O&M operation and maintenance OpenEl Open Energy Information

PL part-load ratio PVs photovoltaics T (K) ambient temperature

TRACI Tool for Reduction and Assessment of Chemicals and

Other Environmental Impacts

Th (kWh) thermal demand

TMY typical meteorological year β_1 first regression coefficient β_2 second regression coefficient

Subscripts

CE conventional energy
DT manufacture data
IV investment
M microturbine
SIM simulation data

References

Arup, 2018. Consumption-based GHG emissions of C40 cities. https://www.c40.org/ researches/consumption-based-emissions.

Baer, P., Brown, M., Kim, G., 2015. The job generation impacts of expanding industrial cogeneration. Ecol. Econ. 110 https://doi.org/10.1016/ j.ecolecon.2014.12.007.

Balcombe, P., Rigby, D., Azapagic, A., 2015a. Energy self-sufficiency, grid demand variability and consumer costs: integrating solar PV, Stirling engine CHP and battery storage. Appl. Energy 155, 393–408. https://doi.org/10.1016/j.apenergy.2015.06.017.

Balcombe, P., Rigby, D., Azapagic, A., 2015b. Environmental impacts of microgeneration: integrating solar PV, Stirling engine CHP and battery storage. Appl. Energy 139, 245–259. https://doi.org/10.1016/j.apenergy.2014.11.034.

Bare, J.C., 2001. TRACI 2.0-The Tool for the Reduction and Assessment of Chemical and Other Environment Impacts. CLEAN TECHNOLOGIES and ENVIRONMENT POLICY, vol. 13. Springer-Verlag, New Yock, NY, pp. 687–696, 5.

Betz, F., 2009. Combined Cooling, Heating, Power, and Ventilation (CCHP/V) Systems Integration. School of Architecture, Carnegie Mellon University. http://citeseerx.ist.psu.edu/viewdoc/download?doi=10.1.1.471. 8112&rep=rep1&type=pdf.

Brandoni, C., Renzi, M., 2015. Optimal sizing of hybrid solar micro-CHP systems for the household sector. Appl. Therm. Eng. 75, 896–907. https://doi.org/10.1016/j.applthermaleng.2014.10.023.

Brooks, W., Dunlop, J., 2012. Photovoltaic (PV) Installer Resource Guide. NABCEP.

Capstone Turbine Corporation, 2009. Product specification model C200-capstone MicroTurbineTM. https://www.regattasp.com/files/460045D_C200_PS.pdf.

Co, K.T.E., 2008. Waste heat energy application for absorption chillers. In: 3rd International Cooling Conference & Trade Show (Dubai, United Arab Emirates).

Darrow, K., Tidball, R., Wang, J., 2017. Catalog of CHP Technologies. US Environmental Protection Agency, Washington. DC. https://www.epa.gov/sites/production/files/2015-07/documents/catalog_of_chp_technologies.pdf.

Faisal, M., Hannan, M.A., Ker, P.J., Hussain, A., Mansor, M.B., Blaabjerg, F., 2018. Review of energy storage system technologies in microgrid applications: issues and challenges. IEEE Access 6, 35143–35164. https://doi.org/10.1109/ACCESS.2018.2841407.

International Fire Code, 2012. IFC 605.11.

James, J.A., Thomas, V.M., Pandit, A., Li, D., Crittenden, J.C., 2016. Water, air emissions, and cost impacts of air-cooled microturbines for combined cooling, heating, and power systems: a case study in the Atlanta region. Engineering 2 (4), 470–480. https://doi.org/10.1016/J.ENG.2016.04.008.

Lee, Dong-Yeon, 2017. Parametric Approach to Life Cycle Assessment. doctoral dissertation. Georgia Institute of Technology, Atlanta, Georgia, the United States.

Lee, D.Y., Thomas, V.M., 2017. Parametric modeling approach for economic and environmental life cycle assessment of medium-duty trucks. J. Clean. Prod. 142 (4), 3300–3321. https://doi.org/10.1016/j.jclepro.2016.10.139.

(4), 3300–3321. https://doi.org/10.1016/j.jclepro.2016.10.139.
Mago, P.J., Chamra, L.M., 2009. Analysis and optimization of CCHP systems based on energy, economical, and environmental considerations. Energy Build. 41, 1099–1106. https://doi.org/10.1016/j.enbuild.2009.05.014.

Mago, P., Fumo, N., Chamra, L., 2009. Performance analysis of CCHP and CHP systems operating following the thermal and electric load. Int. J. Energy Res. 33, 852–864. https://doi.org/10.1002/er.1526.

Maleki, A., Hafeznia, H., Rosen, M.A., Pourfayaz, F., 2017. Optimization of a grid-connected hybrid solar-wind-hydrogen CHP system for residential applications by efficient metaheuristic approaches. Appl. Therm. Eng. 123, 1263–1277. https://doi.org/10.1016/j.applthermaleng.2017.05.100.

Mehrpooya, M., Sayyad, S., Zonouz, M.J., 2017. Energy, exergy and sensitivity analyses of a hybrid combined cooling, heating and power (CCHP) plant with molten carbonate fuel cell (MCFC) and Stirling engine. J. Clean. Prod. 148, 283–294. https://doi.org/10.1016/j.jclepro.2017.01.157.

Mohammadi, A., Ahmadi, M.H., Bidi, M., Joda, F., Valero, A., Uson, S., 2017. Exergy analysis of a Combined Cooling, Heating and Power system integrated with wind turbine and compressed air energy storage system. Energy Convers. Manag. 131, 69–78. https://doi.org/10.1016/j.enconman.2016.11.003.

National Technology and Engineering Solutions of Sandia, LLC., 2018. PVPerformance modeling collaborative. https://pvpmc.sandia.gov/.

PRe North America Inc, 2017. SimaPro.

Rastegar, M., Fotuhi-Firuzabad, M., 2015. Load management in a residential energy hub with renewable distributed energy resources. Energy Build. 107 https://doi.org/10.1016/j.enbuild.2015.07.028.

Rodríguez, L.R., Lissén, J.M.S., Ramos, J.S., Jara, E.Á.R., Domínguez, S.Á., 2016. Analysis of the economic feasibility and reduction of a building's energy consumption and emissions when integrating hybrid solar thermal/PV/micro-CHP systems. Appl. Energy 165, 828–838. https://doi.org/10.1016/j.apenergy.2015.12.080.

Ryberg, M., Vieira, M.D.M., Zgola, M., et al., 2014. Clean Technol. Environ. Policy 16, 329. https://doi.org/10.1007/s10098-013-0629-z.

Shah, K.K., Mundada, A.S., Pearce, J.M., 2015. Performance of U.S. Hybrid distributed energy systems: solar photovoltaic, battery and combined heat and power. Energy Convers. Manag. 105, 71–80. https://doi.org/10.1016/ j.enconman.2015.07.048.

Soheyli, S., Mayam, M.H.S., Mehrjoo, M., 2016. Modeling a novel CCHP system including solar and wind renewable energy resources and sizing by a CC-MOPSO algorithm. Appl. Energy 184, 375–395. https://doi.org/10.1016/ j.apenergy.2016.09.110.

Tesla, Inc, 2017. Tesla Powerwall Limited Warranty (USA).

MATLAB and Statistics Toolbox Release 2018b, The MathWorks, Inc., Natick, Massachusetts, United States.

Torcellini, P., Deru, M., Griffith, K., Benne, B., Halverson, M., Winiarski, D., Crawley.

DOE commercial building benchmark models. Pages 2008, 17-22. https://www.nrel.gov/docs/fy08osti/43291.pdf.

United Nations, 2014. World Urbanization Prospects (2014 Revision).

U.S. Department of Energy, 2018. Combined heat and power installation database, application version 1.1.0. https://doe.icfwebservices.com/chpdb/.

U.S. Department of Energy, 2019. EnergyPlus 9.1.0.

U.S. Department of Energy, National Renewable Energy Laboratory, 2011. Commercial reference building models of the national building stock. https://www.

ARTICLE IN PRESS

J. Yan et al. / Journal of Cleaner Production xxx (xxxx) xxx

nrel.gov/docs/fy11osti/46861.pdf.

U.S. Energy Information Administration, 2019. State profile and energy estimates. https://www.eia.gov/state/?sid=GA.

U.S. Life Cycle Inventory Database, 2012. National renewable energy laboratory, 2012. https://www.lcacommons.gov/nrel/search. (Accessed 19 November

2012).

Yang, Y., Ingwersen, W.W., Hawkins, T.R., Srocka, M., Meyer, D.E., 2017. USEEIO: a new and transparent United States environmentally-extended input-output model. J. Clean. Prod. 158, 308–318. https://doi.org/10.1016/j.jclepro.2017.04.150.

11